Structure, magnetic and transport properties of $(La_{1/2}Sr_{1/2})_{1-x}(Gd_{1/2}Ba_{1/2})_xCoO_3$ perovskites

1999 J. Phys.: Condens. Matter 11 8893

(http://iopscience.iop.org/0953-8984/11/45/312)

J. Phys.: Condens. Matter **11** (1999) 8893–8899. Printed in the UK PII: S0953-8984(99)04282-4

Structure, magnetic and transport properties of $(La_{1/2}Sr_{1/2})_{1-x}$ $(Gd_{1/2}Ba_{1/2})_xCoO_3$ perovskites

J R Sun†‡, Z X Liu†‡ and H K Wong†

† Department of Physics, The Chinese University of Hong Kong, Shatin, Hong Kong, People's Republic of China

‡ State Key Laboratory for Magnetism, Institute of Physics and Centre for Condensed Matter, Chinese Academy of Sciences, Beijing 100080, People's Republic of China

Received 13 May 1999, in final form 15 September 1999

Abstract. Structural, magnetic and transport properties of $(La_{1/2}Sr_{1/2})_{1-x}(Gd_{1/2}Ba_{1/2})_xCoO_3$ with $x = 0$, 0.1, 0.2, 0.3, 0.4, 0.5, 0.6, 0.7, 0.8, 0.9 and 1.0 were experimentally studied. The system exhibits a rhombohedrally distorted perovskite structure for $x \leqslant 0.6$. A rhombohedral–orthorhombic structure transition is induced by the introduction of $Gd_{1/2}Ba_{1/2}$ at $x = 0.7$, resulting in a significant volume contraction of the unit cell. Due to the increased A-cation disorder, the presence of $Gd_{1/2}Ba_{1/2}$ suppresses the ferromagnetic order and enhances the resistivity of the compounds, as demonstrated by the shift of the magnetic transition from ∼255 to ∼160 K for x from 0.0 to 0.8 and the occurrence of the semiconducting conduction for $x \geqslant 0.6$. When the content of $Gd_{1/2}Ba_{1/2}$ exceeds a critical value of ∼0.7, charge ordering occurs and develops below a critical temperature (∼375 K) essentially independent of doping level. It appears that the charge ordering induces the volume contraction of the compounds.

1. Introduction

The half-doped $AMnO_3$-type manganese oxide undergoes a charge ordering (CO) transition, a periodical arrangement of Mn^{3+} and Mn^{4+}, which significantly enhances resistivity and strongly suppressed ferromagnetic (FM) order [1–3]. There is an interesting relation between the CO behaviour and the e_g bandwidth controlled by the A- and B-ion size mismatch in the perovskites [4, 5]. According to their magnetic behaviours, four types of half-doped manganite can be identified: (i) compounds with large tolerance factors ($t = d_{A-O}/\sqrt{2}d_{B-O}$) are ferromagnetic (FM) below the Curie temperature [5], where d_{A-O} and d_{B-O} are the A–O and B–O bond lengths, respectively. (ii) Compounds with a tolerance factor below certain values are A-type antiferromagnetic (AFM). In this case, the double exchange (DE) [6] remains in the a–b plane while spins on neighbouring planes are antiparallel [7]; CO takes place on further weakening of the DE mechanism, and the transition temperature (T_{co}) goes from below T_N (iii) to above T_N (iv) as t decreases [2, 8], where T_N is the critical temperature for the AFM transition. Obviously, the CO occurs at suppressed FM DE interaction [9].

In general, CO is closely correlated with spin and orbital ordering, and its origin is still in dispute. It is supposed that the long-range Coulomb interaction among conduction carriers is responsible for this behaviour [11]. However, in this picture, the significant polaronic character of the charge ordering manifested by the isotope effects [12] and the polaron ordering [13] in this kind of material cannot be explained adequately.

0953-8984/99/458893+07$30.00

There is a suggestion that the cooperative Jahn–Teller (JT) deformation of the MnO_6 octahedra associated with the orbital ordering is determinative to the occurrence of the CO transition [14]. In the perovskite cobaltites, Co^{3+} ($t_{2g}^4e_g^2$), Co^{III+} (t_{2g}^6) and Co^{4+} (t_{2g}^5) are non-JT ions, which may influence the competition between the DE FM, the superexchange AFM and the Coulomb interactions among Co ions and charge carriers. Furthermore, some people believed that the DE is not the only mechanism for the FM ordering in this kind of material [15]. With these in mind, behaviours in the cobaltites could be different from the manganites.

Recently, a CO transition of the type $T_{co} > T_N$ was reported in the half-doped Co-based perovskite $Gd_{1/2}Ba_{1/2}CoO_3$ [10]. The remarkably high transition temperature (∼375 K) manifests the strong tendency of the system to the charge ordered state. It is well known that $La_{1/2}Sr_{1/2}CoO_3$ is FM below the Curie temperature [4]. It is an interesting topic how the system evolves from the latter to the former, and whether or not it experiences other intermediate states as the manganites do.

2. Experiment

Polycrystalline samples $(La_{1/2}Sr_{1/2})_{1-x}(Gd_{1/2}Ba_{1/2})_xCoO_3$ (LSGB) with $x = 0$, 0.1, 0.2, 0.3, 0.4, 0.5, 0.6, 0.7, 0.8, 0.9 and 1.0 were prepared by the conventional solid state reaction method. The mixtures of La_2O_3, Gd_2O_3, $SrCO_3$, $BaCO_3$ and Co_2O_3 powders (with purities higher than 99.9%) of desired ratio were calcined at 900 °C in air for 20 h. The products thus obtained were ground, pelletized and sintered, in oxygen gas flow, at 1250 °C for 5 h followed by an annealing at 1000 °C for 10 h, then furnace cooled to room temperature.

Room temperature powder x-ray diffraction was performed to examine the phase purity and the crystal structure of the samples. Resistance was determined by the standard four-probe technique in the temperature range from 40 to 420 K. Samples used for the measurements were rectangular in shape and about $8\times1\times1$ mm^3 in size. A mutual inductance bridge and a vibrating sample magnetometer were used for the measurements of ac susceptibility and magnetization, respectively.

3. Results

All the samples are of single phase as confirmed by powder x-ray diffraction (XRD). The sample $x = 0.0$ exhibits a rhombohedrally distorted perovskite structure with the lattice constants $a = 5.419$, $c_H = 13.276$ Å. By incorporation of $Gd_{1/2}Ba_{1/2}$ the lattice expands linearly until $x = 0.7$, at which a rhombohedral–orthorhombic structure transition, marked by the dramatic contraction of the unit cell along the orthorhombic c axis, takes place. The volume change of the unit cell due to the structure transition is ∼1.6%, For $x \geqslant 0.7$, the linear increase of a and b remains whereas c diminishes progressively with x, and, finally, for $x = 1.0$, $a = 5.514$, $b = 5.527$ and $c = 7.554$ Å. From $x = 0.6$ to 1.0, the $c/\sqrt{2}a$ (or $c_H/\sqrt{6}a$) ratio reduces from ∼ 1 to ∼0.97. Lattice parameters for the two end members $La_{1/2}Sr_{1/2}CoO_3$ and $Gd_{1/2}Ba_{1/2}CoO_3$ are in good agreement with those reported [16, 17]. Figure 1 shows a typical XRD pattern. The lattice parameters and cell volume as functions of doping level are illustrated in the inset of figure 1. Selected structural parameters are listed in table 1.

Figure 2 presents the temperature dependence of susceptibility (χ) of LSGB. A typical cluster-glass behaviour is observed in $La_{1/2}Sr_{1/2}CoO_3$. The sample is paramagnetic near room temperature. The susceptibility increases steeply at ∼260 K, a sign of FM ordering, then, after an asymmetric maximum, decreases gradually with decreasing temperature. The magnetic transition temperature, defined as the minimum of $d\chi/dT$, shifts downwards progressively by

Table 1. Selected structural parameters of $(La_{1/2}Sr_{1/2})_{0.1}(Gd_{1/2}Ba_{1/2})_{0.9}CoO_3$ determined by the least-squares fitting of the x-ray diffraction profiles in the range $20^\circ \leqslant 2\theta \leqslant 70^\circ$.

x	σ (Å^2)	a (Å)	b (Å)	c (Å)	V (Å^3/Co)
0.0	0.0022	5.419(2)		13.276(3)	56.269
0.1	0.0053	5.419(2)		13.324(3)	56.471
0.2	0.0085	5.446(2)		13.334(3)	57.801
0.4	0.0147	5.457(2)		13.360(3)	57.440
0.5	0.0177	5.454(2)		13.414(3)	57.640
0.6	0.0208	5.474(2)		13.420(3)	57.940
0.7	0.0239	5.470(2)	5.477(2)	7.598(3)	57.908
0.8	0.0269	5.488(2)	5.502(2)	7.567(2)	57.119
0.9	0.0299	5.502(2)	5.519(2)	7.565(3)	57.426
1.0	0.0329	5.514(2)	5.527(2)	7.554(3)	57.545

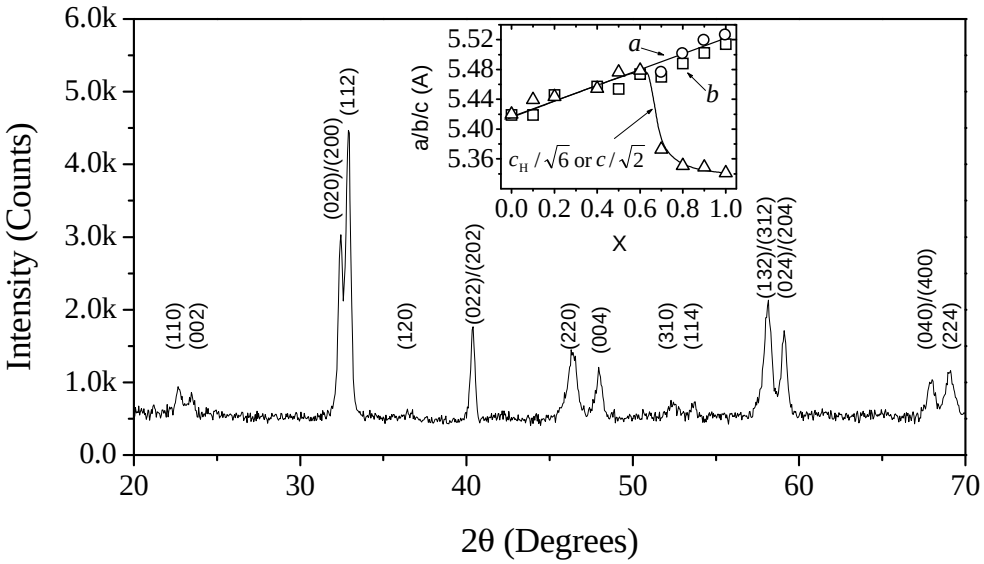

Figure 1. Powder x-ray diffraction pattern for $(La_{1/2}Sr_{1/2})_{0.1}(Gd_{1/2}Ba_{1/2})_{0.9}CoO_3$. Inset: lattice constants as functions of doping level. Error bars are smaller than the symbol size. Solid lines are guides for the eye.

the introduction of $Gd_{1/2}Ba_{1/2}$, accompanying with a tendency to a reduced susceptibility and a broadening transition. A magnetic anomaly emerges and developed at ∼280 K for $x \geqslant 0.7$ (inset in figure 2), while the magnetic state inherited from $La_{1/2}Sr_{1/2}CoO_3$ disappears for $x = 0.9$ and 1.0.

Figure 3 shows the resistivity of LSGB as functions of temperature and doping level. A metallic conduction is exhibited in $La_{1/2}Sr_{1/2}CoO_3$: the resistivity decreases smoothly with decreasing temperature. The FM ordering promotes the conduction of the sample considerably as indicated by the enhanced metallic slope below the Curie temperature. The presence of $Gd_{1/2}Ba_{1/2}$ leads to an increased resistivity and the appearance of semiconductive behaviour as observed in samples with $x \leqslant 0.6$. A small kink at ∼375 K in the ρ–T curve is detected for $x = 0.7$, and it develops into an ambiguous resistivity jump as x approaches 1.0.

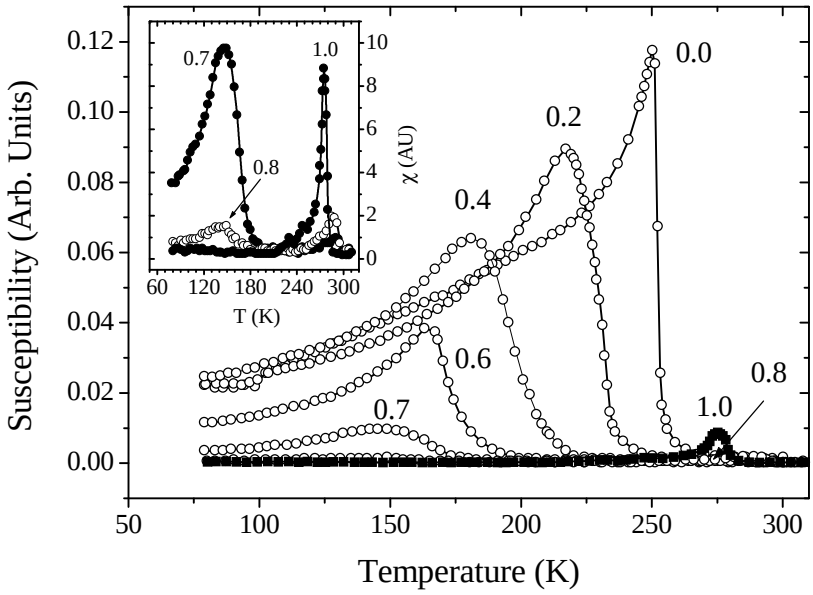

Figure 2. Temperature dependence of susceptibility of $(La_{1/2}Sr_{1/2})_{1-x}(Gd_{1/2}Ba_{1/2})_xCoO_3$ measured at a frequency of 160.2 Hz and a field of 0.4 mT. Inset: details of the susceptibility for samples $x = 0.7$, 0.8 and 1.0. The doping level is labelled by the numbers near the curves.

4. Discussion

The idealized $AMnO_3$ perovskite with $t = 1$ exhibits cubic structure. Generally rhombohedral and orthorhombic structures will be taken subsequently as t decreases. Expansion of the unit cell with x is understandable taking into account the larger ionic size of $Gd_{1/2}Ba_{1/2}$ compared to $La_{1/2}Sr_{1/2}$ [18]. However, it is interesting that $Ga_{1/2}Ba_{1/2}CoO_3$ with a larger tolerance factor exhibits a lower symmetry according to the present investigations. An important difference between $La_{1/2}Sr_{1/2}CoO_3$ and $Gd_{1/2}Ba_{1/2}CoO_3$ is the substantial A-ion disorder in the latter. A simple calculation gives the variances of the A-cation radius distribution, $\sigma^2 = \sum x_i r_i - \langle r_A^2 \rangle$, for both compounds: 0.0022 for $x = 0.0$ and 0.0329 Å^2 for $x = 1.0$, where r_A is the average A-site cation radius; r_i and x_i are ionic radius and fractional occupancy of ion A_i, respectively. The A-ion disorder can enhance the CoO_6 deformations due to the random displacements of oxygen, inducing the rhombohedral–orthorhombic transition [19].

From figures 1 and 2, the structural discontinuity and the magnetic anomaly take place at a similar doping level $x = 0.7$. These behaviours are clearly a consequence of the CO according to the resistivity measurements. The CO could localize the conduction carriers, leading to the discontinuous resistive slopes around the transition. Usually, the CO favours a cooperative structure deformation, which shrinks the unit cell along the orthorhombic c axis, reducing the $c/\sqrt{2}a$ ratio. Iodometric titration shows similar Co^{4+}/Co content of 0.47 ± 0.02 for all the samples. Therefore, this structure change cannot be a result of O deficiency. As a matter of fact, these are typical structure characters of the CE-type AFM perovskites suggested by Goodenough [20]. A similar rhombohedral–orthorhombic structure transition was also observed in the half-doped manganese oxides except for a slightly smaller volume contraction of ∼0.1% upon the CO transition [8]. In the manganite, Mn^{3+} is a strong JT ion, which can distort the MnO_6 octahedra and trap the e_g electron at the Mn^{3+} site and thus weaken the

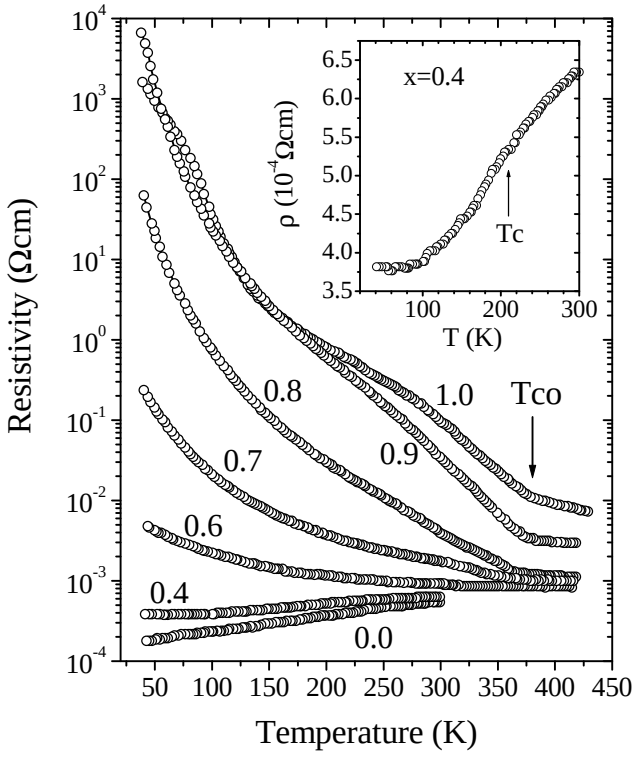

Figure 3. Temperature dependence of resistivity of $(La_{1/2}Sr_{1/2})_{1-x}(Gd_{1/2}Ba_{1/2})_xCoO_3$. The doping level is labelled by the numbers near the curves. The arrow marks the temperature for the charge ordering transition (T_{co}). Inset: details of the resistivity of the sample $x = 0.4$. T_c is the temperature for the magnetic transition.

DE process. With the help of this effect, the Coulomb repulsion among conduction carriers drives the system into the charge-ordered state. In contrast, Co^{3+}, Co^{III+} and Co^{4+} are non-JT ions. The substantial A disorder distorts the CoO_6 octahedra, which may not be the JT-type distortion, in $Gd_{1/2}Ba_{1/2}CoO_3$. This may be the underlying mechanism driving the system to the charge ordered state. It is obvious that the A-ion disorder suppresses strongly the DE coupling between Co^{3+} and Co^{4+}, as demonstrated by a monotonic shift to lower temperatures of the Curie temperature with x, helping to localize the conduction carriers. The present investigation suggests that the JT effects are not necessary for CO transition. The tolerance factor of the compound increases slightly with x, which disfavours the CO state. However, its effect is counteracted by that from the A disorder. It is interesting to note that the CO sets in for LSGB at $\sigma^2 = 0.0239$ Å, while for $R_{1/2}Ba_{1/2}CoO_3$ (R = rare earth atom) an alternative series shows the CO transition at $\sigma^2 = 0.0236$ Å [17]. The disfavour of the CO to the FM order is also shown by the rapid reduction of the magnetization after the CO transition (figure 4).

The abrupt structure change indicates clearly the CO onset. According to the structural, magnetic and transport studies, CO appears for $x \geqslant 0.7$ at temperatures essentially independent of doping level. This is different from the observations in $R_{1/2}Ba_{1/2}CoO_3$ (R = rare earth atoms), in which it is reported that T_{co} shifts to lower temperatures with the size of R until $T_{co} \sim 250$ K for R = Nd [17].

For the half-doped manganese oxides, several intermediate states appear between the charge disordered FM $La_{1/2}Sr_{1/2}MnO_3$ and the charge ordered AFM $Pr_{1/2}Ca_{1/2}MnO_3$.

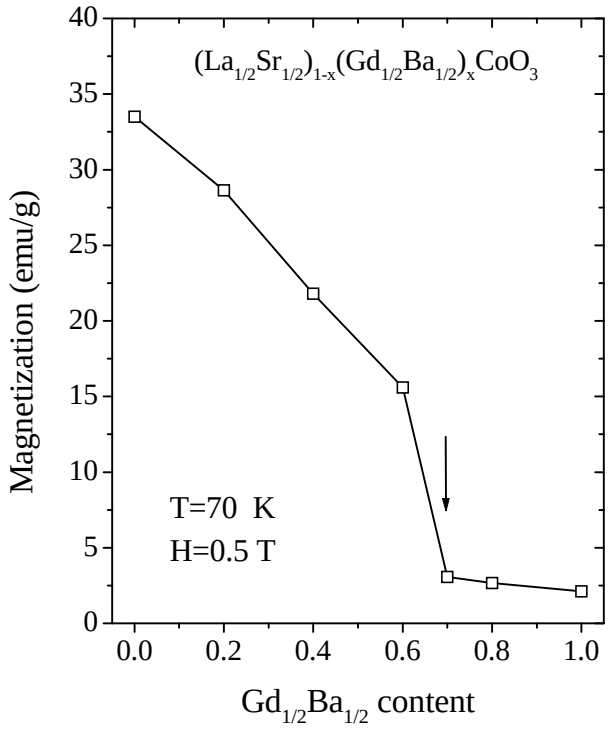

Figure 4. Magnetization of $(La_{1/2}Sr_{1/2})_{1-x}(Gd_{1/2}Ba_{1/2})_xCoO_3$ as a function of doping level. The arrow indicates the critical content of $Ga_{1/2}Ba_{1/2}$ for charge ordering. The solid line is a guide to the eye.

With decreasing the e_g bandwidth, the DE interaction among neighbouring c planes diminishes, forming the A-type AFM state. CO emerges when the DE is further weakened. The critical temperatures T_{co} goes from below to above T_N as the tolerance factor decreases. The tendency to the CO state enhances at the expense of the DE mechanism.

The CO observed in $Gd_{1/2}Ba_{1/2}CoO_3$ satisfies $T_N < T_{co}$. We failed to reproduce the intermediate states similar to those occurred in the manganites by simply enhancing the A-ion disorder that controls the FM coupling between Co ions. Instead, the system goes directly from the FM to the charge ordered AFM state at a critical substitution ($x = 0.7$) of $Gd_{1/2}Ba_{1/2}$ for $La_{1/2}Sr_{1/2}$. Fascinatingly, a weak FM–AFM transition emerges and develops above $x = 0.7$ (inset in figure 2). Further investigations are required to reveal its underlying physics.

5. Summary

In summary, the structural, magnetic and transport properties of $(La_{1/2}Sr_{1/2})_{1-x}(Gd_{1/2}Ba_{1/2})_x$ CoO_3 with $x = 0$, 0.1, 0.2, 0.3, 0.4, 0.5, 0.6, 0.7, 0.8, 0.9 and 1.0 were experimentally studied. The system exhibits a rhombohedrally distorted perovskite structure for $x \leqslant 0.6$. A rhombohedral–orthorhombic structure transition is induced by the introduction of $Gd_{1/2}Ba_{1/2}$ at $x = 0.7$, resulting in a significant volume contraction of the unit cell. The presence of $Gd_{1/2}Ba_{1/2}$ suppresses the ferromagnetic order and enhances the resistivity of the compounds, as demonstrated by the shift of the magnetic transition from ∼255 to ∼160 K for x from 0.0

to 0.8 and the occurrence of the semiconducting conduction for $x \geqslant 0.6$. When the content of $Gd_{1/2}Ba_{1/2}$ exceeds a critical value ~ 0.7, charge ordering occurs and develops below a critical temperature ($\sim$375 K) essentially independent of doping level. The increased A-cation disorder due to the incorporation of $Gd_{1/2}Ba_{1/2}$ may be responsible for the observed behaviours. The present investigation also suggests that the Jahn–Teller effects are not necessary for the charge ordering transition.

Acknowledgment

This work was supported by the Hong Kong Research Grant Council, the Croucher Foundation and the State Key Project for Elementary Research of China. Z X Liu was supported by the C N Yang visiting fellowship fund.

References

[1] Tomioka Y, Asamitsu A, Moritomo Y, Kuwahara H and Tokura Y 1995 *Phys. Rev. Lett.* **74** 5108
[2] Kuwahara H, Tomioka Y, Asamitsu A, Moritomo Y and Tokura Y 1995 *Science* **270** 961
[3] Tomioka Y, Asamitsu A, Kuwahara H, Moritomo Y and Tokura Y 1996 *Phys. Rev.* B **53** R1689
[4] Damay F, Martin C, Maignan A and Raveau B 1997 *J. Appl. Phys.* **82** 6181
[5] Sundaresan A, Paulose P L, Mallik R and Sampathkumaran E V 1998 *Phys. Rev.* B **57** 2690
[6] Zener C 1951 *Phys. Rev.* **82** 403
Anderson P W and Hasagawa H 1955 *Phys. Rev.* **100** 675
de Gennes P-G 1960 *Phys. Rev.* **118** 141
[7] Kawano H, Kajimoto R, Yoshizawa H, Tomioka Y, Kuwahara H and Tokura Y 1997 *Phys. Rev. Lett.* **78** 4253
[8] Moritomo Y, Kuwahara H, Tomioka Y and Tokura Y 1997 *Phys. Rev.* B **55** 7549
[9] Kuwahara H, Moritomo Y, Tomioka Y, Asamistu A, Kasai M, Kumai R and Tokura Y 1997 *Phys. Rev.* B **56** 9386
[10] Troyanchuk I O, Kasper N V, Khalyavin D D, Szymczak H, Szymczak R and Baran M 1998 *Phys. Rev. Lett.* **80** 3380
[11] Anisimov V I, Elfimov I S, Korotin M A and Terakura K 1997 *Phys. Rev.* B **55** 15 494
Mishra S K, Pandit R and Satpathy S 1997 *Phys. Rev.* B **56** 2316
Sheng L and Ting C S 1997 *Phys. Rev.* B **57** 5265
[12] Zhao G M, Ghosh K, Keller H and Greene R L 1999 *Phys. Rev.* B **59** 81
[13] Li J Q, Uehara M, Tsuruta C, Matsui Y and Zhao Z X 1999 *Phys. Rev. Lett.* **82** 2386
Yamada Y, Hino O, Nohdo S, Kanao R, Inami T and Katano S 1996 *Phys. Rev. Lett.* **77** 904
[14] Mizokawa T and Fujimoti A 1997 *Phys. Rev.* B **56** R493
Ahn K H and Millis A J 1998 *Phys. Rev.* B **58** 3697
[15] Senaris-Rodriguez M A and Goodenough J B 1995 *J. Solid State Chem.* **118** 323
[16] Mineshige A, Inaba M, Yao T and Ogumi Z 1996 *J. Solid State Chem.* **121** 423
[17] Moritomo Y, Takeo M, Liu X J, Akimoto T and Nakamura A 1998 *Phys. Rev.* B **58** R13 334
[18] Shannon R D 1976 *Acta Crystallogr.* A **32** 751
[19] Rodriguez-Martinez L M and Attfield J P 1996 *Phys. Rev.* B **54** R15 622
[20] Goodenough J B 1951 *Phys. Rev.* **100** 505